Relationships between conductivity and local topology in heterocyclic polymer networks

V. Yu. Kramarenko,[1] T. A. Ezquerra,[2] and V. P. Privalko[3]
[1]*State Polytechnic University, Frunze 21, 61002 Kharkiv, Ukraine*
[2]*Instituto de Estructura de la Materia, CSIC, Serrano 119, 28006 Madrid, Spain*
[3]*Institute of Macromolecular Chemistry, National Academy of Sciences of Ukraine, Kharkiv Chaussee 48, 02160 Kyiv, Ukraine*
(Received 24 October 2002; published 12 March 2003)

The low frequency complex dielectric relaxation above the glass transition temperature T_g for a series of well-characterized heterocyclic polymer networks has been analyzed in terms of the electric moduli formalism. It was established that the contribution of ionic conductivity to the electric modulus can be quantitatively separated from the α relaxation by using a combination of two Havriliak-Negami (HN) functions. A strong correlation between the mechanisms of both conductivity and segmental mobility was inferred from the similarity of the shape of the HN function for conductivity relaxation to those for the main relaxation. This correlation is further supported by the similarity of the temperature dependencies of the relevant relaxation times corresponding to both processes. The overwhelming contribution of the preexponents D_0 in the Arrhenius behavior of the apparent diffusion coefficients can be explained by considering a model implying decreased mean free paths of the diffusing elements and lower activation entropies of diffusion for polymer networks with higher apparent network densities.

DOI: 10.1103/PhysRevE.67.031801 PACS number(s): 61.41.+e, 64.70.Pf

I. INTRODUCTION

The onset of ionic conductivity for many polymers manifests itself as a sudden rise of both real (ε') and imaginary (ε'') components of the complex dielectric function ε^* upon approaching the glass transition. Such a behavior is usually associated with the generation and transport of polarization-induced charges through the polymer matrix under the action of an electric field. The complex conductivity σ^* is related to ε^* through $\sigma^*=\sigma'+i\sigma''=i\omega\varepsilon_0\varepsilon^*$, where ε_0 is the dielectric permittivity of the vacuum and ω is the angular frequency. Accordingly, the real part of the conductivity can be measured as $\sigma'=\varepsilon''\omega\varepsilon_0$. The recognition of the complex dielectric function ε^* as a compliance allows one to define an electric modulus as

$$M^*=\frac{1}{\varepsilon^*}=\frac{\varepsilon'}{\varepsilon'^2+\varepsilon''^2}+i\frac{\varepsilon''}{\varepsilon'^2+\varepsilon''^2}=M'+iM''. \quad (1)$$

By using the electric modulus formalism for the treatment of dielectric data an enhancement of the contribution of conductivity effects can be obtained [1,2]. The major weakness of this formalism arises from the fact that the electric modulus is not a directly measurable property [3]. However, as far as conductive effects are concerned, this is counterbalanced by the following obvious advantages: (i) In contrast to the relatively smooth patterns of $\varepsilon''(\omega)$ plots, the electric loss moduli $M''(\omega)$ exhibit relaxation maxima which can be characterized by corresponding relaxation times and shape factors; (ii) the contribution of electrode screening effects in the low-frequency spectrum tail can be eliminated.

Currently, the modulus formalism is widely used in the data treatment for ion-conducting glasses to derive the mean relaxation times, the Kohlrausch-Williams-Watts (KWW) stretching exponents β_{KWW}, and the apparent activation energies for conductivity E_σ [1–10]. Semiquantitative correlations between β_{KWW} and E_σ, as well as between these parameters and the mean interionic distances, have been reported [5,6].

Although the mechanism of electrical conduction in polymers is an important issue, the explicit use of the modulus formalism is a relatively new topic in this field [11,12]. In particular, studies aiming to look for relationships between the conduction mechanism and the molecular structure are scarce. This is partly due to the fact that conductivity manifests itself as an undesirable low-frequency increment in ε^* which usually masks the more intensively studied relaxational processes. Recently, the modulus formalism was applied to evaluate conductivity effects in polymers like polyethylene terephthalate [13,14], nylon-11 [15,16], polyether imide [17], and segmented polyurethanes [18–20]. As far as polymer networks are concerned, the apparent conductivity estimated from the modulus formalism has been proved to be a useful measure of chemical conversion in epoxy-amine networks [11,21,22]. In particular, for model heterocyclic polymer networks a direct relation between both local and segmental dynamics and the network topology has been found. However, a possible relation between conductivity effects and network topology has not been established. In this paper, the modulus formalism is used to discuss the structural implications of conductivity for a series of well-characterized heterocyclic polymer networks (HPNs) in order to gain a deeper knowledge about the conduction mechanism of polymer networks. The general aim of our study is to seek for relationships between the system topology, particularly the degree of cross linking and the conduction behavior.

II. EXPERIMENT

Heterocyclic polymer networks were prepared by curing mixtures of hexamethylene diisocyanate and hexyl isocyanate with different ratios as described elsewhere [23,24]. By

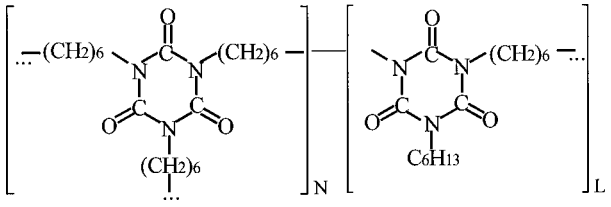

FIG. 1. Generalized chemical scheme of heterocyclic polymer networks.

this procedure, regularly cross-linked copolymers are obtained with precise molar fractions of three-arm (cross-linked) and two-arm (linear) segments (Fig. 1). Assuming full conversion of the reaction groups and formation of a defect-free network structure some relevant structural parameters can be calculated (Table I). Here, L/N refers to the relative ratio of linear and network structures (Fig. 1), M_c is the average molecular weight of chain strands between two cross links, P is the molar content of NCO groups in the copolymers, and T_g is the glass transition temperature as determined by differential scanning calorimetry [23]. An important feature of these systems is an almost invariant concentration of dielectrically active components in spite of significant topology variation. The complex dielectric permittivity $\varepsilon^* = \varepsilon' - i\varepsilon''$ was measured covering a frequency range $10^{-1} < F < 10^5$ Hz by using a Standford lock-in amplifier SR830 with a dielectric interface and control temperature unit from Novocontrol as previously described [23,24].

III. RESULTS

In a first step, the complex dielectric functions in the temperature intervals above the glass transition temperatures T_g for all studied HPNs were converted into electric moduli through Eq. (1). As can be seen from the representative plot for the sample with the maximum cross-link density (Fig. 2), the electric loss modulus M'' passes through three relaxation maxima which can be identified, in line with the accepted nomenclature [25], as the β, α, and σ processes, respectively, in the order of increasing temperature.

The next step involved subsequent treatment of the data for isothermal conditions. In view of significant distortions of the conductivity-dominant process due to the α relaxation upon approaching the main relaxation at $T_a \approx T_g$, the data were described by a combination of two Havriliak-Negami

TABLE I. Parameters of investigated systems: L/N, relative ratio of linear to network content; M_c, average molecular weight of segment between two cross links; P, content of NCO polar groups; T_g, glass transition temperature.

L/N	M_c (g/mol)	P (%)	T_g (K)
100/0		42.7	287.6
75/25	1137.0	44.3	310.1
60/40	694.5	45.4	324.6
43/57	473.3	46.6	337.1
0/100	252.0	50.0	362.0

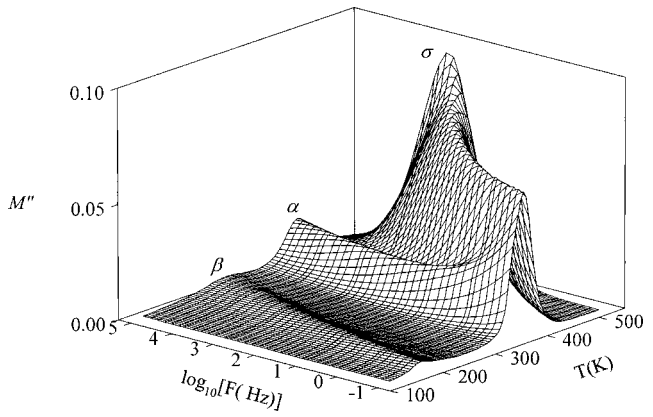

FIG. 2. M'' as a function of temperature and frequency for sample with $L/N = 0/100$.

(HN) functions [26] for both $M'(F)$ and $M''(F)$:

$$M^* = M_\infty - \frac{\Delta M_1}{[1+(i\omega\tau_\sigma)^{b1}]^{c1}} - \frac{\Delta M_2}{[1+(i\omega\tau_\alpha)^{b2}]^{c2}}, \quad (2)$$

where τ_σ and τ_α are the mean relaxation times for σ and α processes, respectively, 1 and 2 are the corresponding indices, and the physical meaning of other relevant parameters can be derived from Fig. 3. The limiting value of the real part of the complex modulus at $F \to \infty$ is obviously $M_\infty = 1/\varepsilon_{\alpha,\infty}$; since $1/\varepsilon_{\sigma,\infty} \to 0$ in the limit $F \to \infty$, the standard definition $\Delta M_1 = 1/\varepsilon_{\alpha,0} - 1/\varepsilon_{\sigma,\infty}$ can be reduced to $\Delta M_1 \approx 1/\varepsilon_{\alpha,0}$; finally, $\Delta M_2 = 1/\varepsilon_{\alpha,\infty} - 1/\varepsilon_{\alpha,0}$.

The excellent quality of the data fits for all studied samples can be assessed from Figs. 4(a) and 4(b). The best-fit values of the parameters of Eq. (2) are presented in Table II. It can be easily verified that the values related to α relaxation compare well with those derived in our previous work [23].

As mentioned above, the onset of ionic conductivity is associated with the generation and diffusion of polarization-induced charges through a polymer matrix under the action of electric field. The Trukhan model of polarization in het-

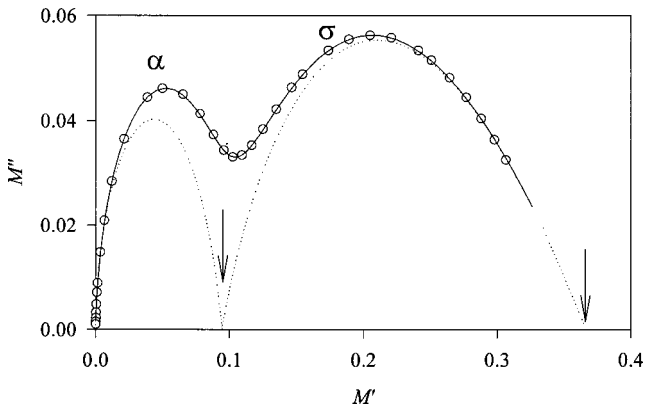

FIG. 3. Complex plane plot for electrical modulus at 343 K for $L/N = 100/0$. The continuous line represents the best fit for the sum of two HN functions (dotted lines). The arrows indicate the limiting values for the σ and α relaxations (see text).

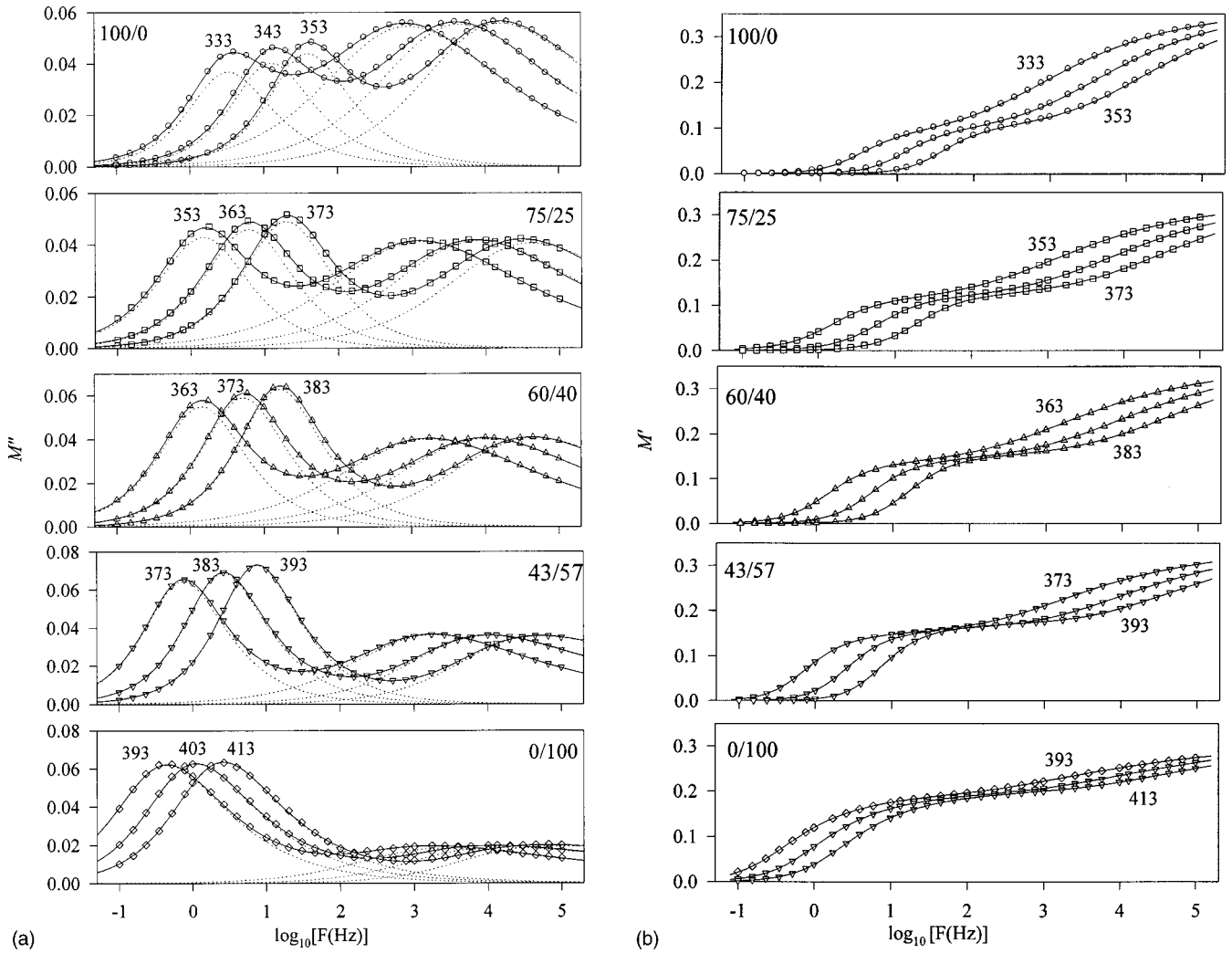

FIG. 4. M'' (a) and M' (b) spectra of the HPN system obtained at different temperatures. The continuous lines represent the best fits for the sum of two HN functions (dotted lines).

TABLE II. Parameters obtained from the fitting of Eq. (2).

L/N	T (K)	ΔM_1	b_1	c_1	$\tau_{0\sigma}$ (s)	ΔM_2	M_∞
100/0	333	0.088	0.970	0.743	6.14×10^{-2}	0.274	0.362
	343	0.095	0.968	0.781	1.56×10^{-2}	0.276	0.370
	353	0.103	0.965	0.788	4.91×10^{-3}	0.282	0.385
75/25	353	0.109	0.998	0.847	1.08×10^{-1}	0.223	0.331
	363	0.115	0.996	0.860	2.63×10^{-2}	0.221	0.335
	373	0.121	0.995	0.878	8.41×10^{-3}	0.221	0.342
60/40	363	0.133	0.896	0.940	1.18×10^{-1}	0.223	0.357
	373	0.142	0.914	0.901	3.30×10^{-2}	0.224	0.365
	383	0.150	0.925	0.875	1.10×10^{-2}	0.220	0.369
43/57	373	0.152	0.957	0.809	2.50×10^{-1}	0.196	0.366
	383	0.162	0.962	0.795	7.22×10^{-2}	0.205	0.386
	393	0.171	0.973	0.776	2.60×10^{-2}	0.243	0.414
0/100	393	0.199	0.828	0.630	5.72×10^{-1}	0.131	0.326
	403	0.200	0.863	0.573	2.46×10^{-1}	0.171	0.370
	413	0.204	0.869	0.570	1.07×10^{-2}	0.203	0.433

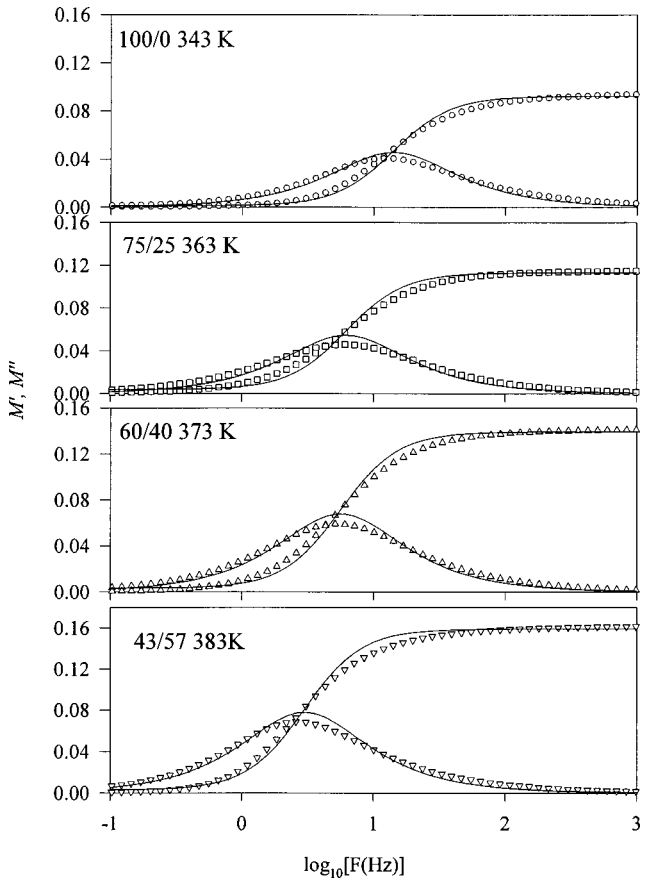

FIG. 5. M^* vs frequency for the model predicted by Eq. (3) for temperatures obtained for the condition $T \approx T_g + 50$ K for each sample. Symbols the same as in Fig. 4.

erogeneous systems comprising several layers with different dielectric permittivities [27] was shown to be useful to derive the relevant diffusion coefficients D for a copolymer of vinyl acetate and vinylidene cyanide [28]. More recently, the conductivity effects in polyetherimide were treated by a more refined version of the Trukhan model in which the contribution of diffusion to the real and imaginary components of complex dielectric function were accounted for by the following approximate relationships [17]:

$$\varepsilon' \approx \frac{\lambda/d + \omega^2\tau^2(1-3\lambda/8d)}{\lambda^2/d^2 + \omega^2\tau^2(1-\lambda/d)}, \tag{3a}$$

$$\varepsilon'' \approx \frac{\omega\tau(1-3\lambda/2d)}{\lambda^2/d^2 + \omega^2\tau^2(1-\lambda/d)}, \tag{3b}$$

where d is the distance between electrodes (i.e., sample thickness), τ is the characteristic time of the $M''(F)$ maximum, and λ is defined as

$$\lambda = \sqrt{D\tau}. \tag{4}$$

The apparent diffusion coefficients D were estimated from Eq. (4) using the parameters λ and τ derived from the best fit of the HN function data of the conduction process to Eqs. (3a) and (3b). A representative example of the best fit of the latter model to the low-frequency conductivity-dominated data derived through Eq. (3) is shown in Fig. 5 for samples with different cross-link densities at selected temperatures.

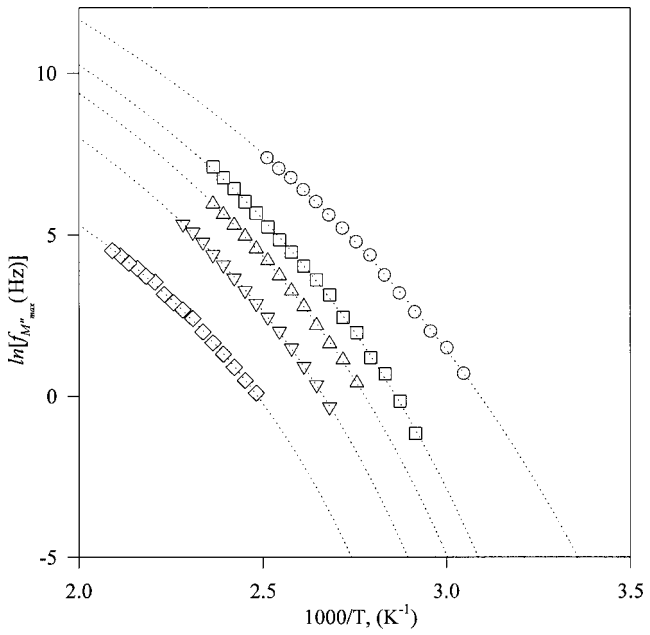

FIG. 6. $f_{M''_{\max}}$ as a function of the reciprocal temperature for HPN systems with different L/N ratios. The lines are best fits of Eq. (5). Symbols the same as in Fig. 4.

IV. DISCUSSION

A. Shape factors

As can be inferred from the data collected in Fig. 4 and in Table II, in the modulus representation the values of the shape factors b and c for the conductivity relaxation (σ) are closer to unity. This indicates that the corresponding maxima are more symmetric and narrower than those of the main transition (α), although for both processes these parameters decrease with increasing apparent network density [23]. The temperature dependence of the frequencies corresponding to the σ relaxation which can be extracted from the maxima of $M''(F)$ can be analyzed in terms of the Vogel-Tammann-Fulcher (VTF) equation

$$f_{M''_{\max}} = f_0 \exp\left(-\frac{B}{T-T_0}\right), \tag{5}$$

where f_0 is the preexponential factor, T_0 ($<T_g$) is usually considered as a hypothetical temperature of the second-order transition, and the parameter B is related to the liquid "strength" parameter D_s through $B = D_s T_0$ [29]. The quality of the data fits for all studied samples can be assessed from Fig. 6. The best-fit values of the parameters of Eq. (5) are presented in Table III. The data obtained clearly indicate a non-Arrhenius behavior of $f_{M''_{\max}}$ similar to the relaxation times derived from Eq. (2). Moreover, the VFT parameters derived from Eq. (5) for the conductivity process are in excellent agreement with those previously calculated for the α

TABLE III. Best-fit parameters for $f_{M''_{max}}(T)$ of electric modulus (Fig. 6).

L/N	f_0 (Hz)	B (K)	T_0 (K)	D_s
100/0	5.53×10^8	2584	195.1	13.25
75/25	8.95×10^7	2164	231.1	9.37
60/40	4.45×10^7	2158	237.5	9.09
43/57	1.06×10^7	2051	248.6	8.25
0/100	2.63×10^5	1641	270.9	6.06

relaxation (Table 3 in Ref. [23]). This indicates that for both processes the limiting temperature T_0 increases, while the strength parameter D_s decreases, the higher the network density. Apparently, the mobilities of both HPN segments and charge carriers become completely suppressed at the same limiting temperature. It should be emphasized, however, that in contrast to the data treatment of segmental mobility in the glass transition interval where a universal, fixed value $f_0 = 10^{14}$ Hz has been recommended as a limiting frequency of elementary oscillations [30], an equivalent universal value for the excitations of charge carriers can hardly be expected. Stated otherwise, the intrinsic frequency of conductivity relaxation at very high temperatures should be different from that for elementary chain oscillations.

B. Conductivity behavior

The conductivity values evaluated through $\sigma' = \varepsilon'' \varepsilon_{vac} \omega$ are plotted vs frequency F for isothermal conditions at $T = 398$ K [Fig. 7(a)]. Qualitatively, the experimental behavior of σ' with frequency can be accounted for by the general expression $\sigma' = \sigma_{dc} + C(\omega/2\pi)^s$, where C is a constant, as observed in glassy and molten ionic conductors [31,32]. The values of the exponent s were below unity and tend to decrease with increasing apparent network density [23]. Theoretically, $s<1$ is predicted for a system with a broad distribution of conductivity relaxation times [2]. Figure 7(a) shows that higher conductivity levels are observed for a linear polymer ($L/N = 100/0$), while the fully cross-linked system ($L/N = 0/100$) exhibits values lower by nearly 3.5 orders of magnitude. Similar plots at equivalent $T_g + 50$ K overheating above the respective glass transition temperatures for different samples are shown in Fig. 7(b). Under these conditions the electrode screening effects, which manifest themselves as a broad hump on the plot in Fig. 7(a) for the linear sample, are eliminated. As in the previous case [Fig. 7(a)], the conductivity levels are higher for the linear polymer than for the fully cross-linked system.

C. Diffusion coefficients

As shown in Fig. 5, the experimental data in the conduction region (σ process) taken at analogous overheatings $T \approx T_g + 50$ K can be adequately described by means of the Trukhan model which explicitly takes into account the diffusion mechanism of the charge carrier transport. The small deviations of the experimental data from the predicted model can result from neglecting the finite relaxation time spectrum

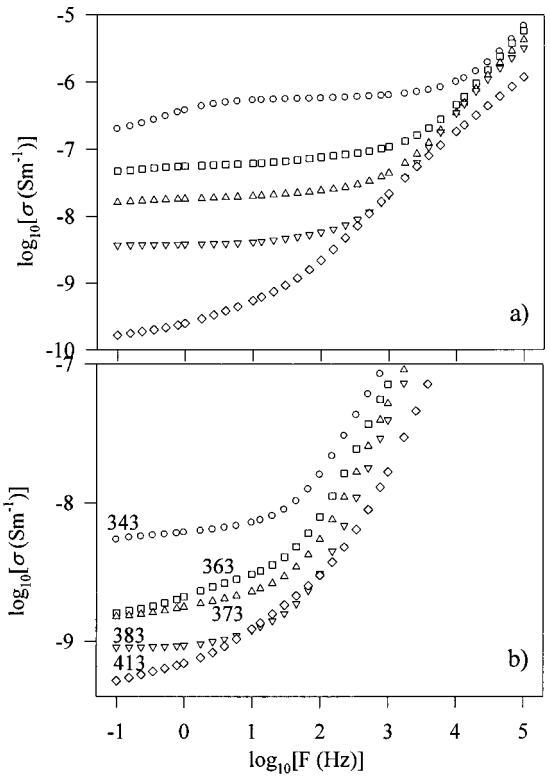

FIG. 7. Conductivity vs frequency plots at 398 K (a) and for different temperatures, obtained for the condition $T \approx T_g + 50$ K for each sample (b). Symbols the same as in Fig. 4.

in the diffusion model [17]. However, due to the relatively small deviations from unity of the shape parameters b_1 and c_1 calculated by Eq. (2) (Table II), it seems reasonable to consider this model in a first approximation to estimate the apparent diffusion coefficients D for the studied samples. We exclude from this treatment the fully cross-linked sample due to its remarkable asymmetry and the broadening of the distribution.

As inferred from Fig. 8, the diffusion coefficients follow an Arrhenius-like temperature dependence according to Eq. (6):

$$D = D_0 \exp\left(-\frac{E_D}{RT}\right). \tag{6}$$

Here, E_D is the apparent activation energy of diffusion and D_0 is the preexponential factor. The Arrhenius behavior of D might seem somewhat surprising, in so far as both $f_{M''_{max}}$ and τ exhibited the VFT behavior. It should be remarked, however, that the apparent diffusion coefficients D were calculated by Eq. (4), which is a special combination of the parameters τ and λ, each exhibiting the VTF behavior. Therefore, there is no *a priori* reason that D should also behave in a VFT-like way, although this issue can be settled only after measurements over broader temperature intervals.

The best-fit parameters of Eq. (6) are shown in Table IV. The observed decrease of E_D with the increasing network density (Table IV) is somewhat at variance with the expected behavior [33]. However, it can easily be verified that in all

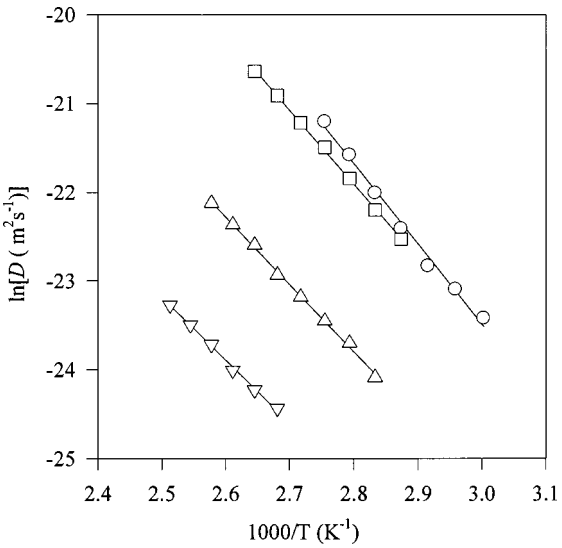

FIG. 8. Arrhenius plot of diffusion coefficients for HPN systems with different L/N ratios. The straight lines are best fits of Eq. (6). Symbols the same as in Fig. 4.

cases the differences between the apparent diffusion coefficients for samples with different L/N ratios decrease with decreasing temperature, until an approximately similar value of $D_g = 10^{-12} - 10^{-13}$ m^2/s is reached at the corresponding glass transition temperatures T_g. Thus, the relatively minor effect of different E_D on D is overbalanced by the overwhelming contribution of the difference (by several orders of magnitude) between preexponents D_0.

The simplest model of diffusion [33] assumes that the preexponent D_0 in Eq. (6) is related to the diffusive free path λ_D and to the activation entropy S_D as

$$D_0 \sim \lambda_D^2 \exp(S_D/k). \tag{7}$$

In this context, the observed fall of D_0 with the apparent network density can be associated, formally, with the decrease of either λ_D or S_D. Within the frame of the energy landscape model, the activation entropy $S_D = S^* - S_0$ is a measure of structural perturbations occurring by the temporary visits of relevant kinetic units initially located in energy valleys of entropy S_0 to activated states of entropy S^*. In our case, for polymer networks, the activated state can be envisioned as a perturbed network structure enabling direct transport of the diffusing elements. Compared with the initial unperturbed state, this perturbation could imply the stretching of chain strands of mean molar mass $\langle M_c \rangle$ between network junctions. This process will be opposed by an entropic resistance which should increase with increasing network density as the reciprocal of $\langle M_c \rangle$. Hence, the mean free path λ_D should also decrease with increasing network density. This effect, however, is expected to be too small to account for the observed changes of D_0 by several orders of magnitude. Assuming that $S^* \approx$ const for all samples, the additional fall of D_0 may be explained only by the contribution of the exponential term due to the decrease of S_D resulting from a progressively looser packing (that is, higher S_0) of the unperturbed state as network density increases. This assumption is consistent with the previous report of β relaxation in these model polymer networks [24]. In this study, a looser molecular packing with increasing network densities caused by the increasing content of loosely packed network junctions due to the six-member, three-arm isocyanurate rings was invoked in order to explain the behavior of the β process.

TABLE IV. Activation energies and preexponential factors of diffusion coefficients.

L/N	E_D (kJ mol^{-1})	D_0 (m^2/s)
100/0	75.37	4.131×10^{1}
72/25	69.42	4.412×10^{0}
60/40	63.13	7.963×10^{-2}
43/57	58.57	3.820×10^{-3}

V. CONCLUSIONS

(1) The contribution of conductivity to the electric modulus of heterocyclic polymer networks can be quantitatively separated from the contribution of the main α-relaxation process by using combination of two HN functions.

(2) The Trukhan model can be used to extract from the experiments the apparent diffusion coefficients.

(3) The similarities of the temperature dependences of relaxation times for the conduction process (σ) and for the main relaxation (α) suggest a strong correlation between the mechanisms of conductivity and segmental mobility.

(4) The overwhelming contribution of the preexponents D_0 to the Arrhenius behavior of the apparent diffusion coefficients can be explained by considering a model implying decreased mean free paths of the diffusing elements and lower activation entropies of diffusion for polymer networks with higher apparent network densities.

ACKNOWLEDGMENT

The authors acknowledge financial support from the MCYT (Grant No. FPA2001-2139), Spain, for generous support of this investigation.

[1] C. T. Moynihan, R. D. Bressel, and C. A. Angell, J. Chem. Phys. **55**, 4414 (1971).
[2] P. B. Macedo, C. T. Moynihan, and R. Bose, Phys. Chem. Glasses **13**, 171 (1972).
[3] S. R. Elliott, J. Non-Cryst. Solids **170**, 97 (1994).
[4] C. T. Moynihan, L. P. Boesch, and N. L. Laberge, Phys. Chem. Glasses **14**, 122 (1973).
[5] K. L. Ngai and S. W. Martin, Phys. Rev. B **40**, 10 550 (1989).
[6] H. K. Patel and S. W. Martin, Phys. Rev. B **45**, 10 292 (1992).
[7] D. L. Sidebottom, P. F. Green, and R. K. Brow, J. Non-Cryst.

Solids **183**, 151 (1995).
[8] C. T. Moynihan, Solid State Ionics **105**, 175 (1998).
[9] B. Roling, Solid State Ionics **105**, 185 (1998).
[10] A. Pimenov, J. Ullrich, P. Lunkenheimer, A. Loidl, and C. H. Ruscher, Solid State Ionics **109**, 111 (1998).
[11] M. B. M. Mangion and G. P. Johari, J. Polym. Sci., Part B: Polym. Phys. **28**, 1621 (1990).
[12] H. W. Starkweather and P. Avakian, J. Polym. Sci., Part B: Polym. Phys. **30**, 637 (1992).
[13] E. Neagu, P. Pissis, L. Apekis, and J. L. Gomez Ribelles, J. Phys. D **30**, 1551 (1997).
[14] E. Neagu, P. Pissis, and L. Apekis, J. Appl. Phys. **87**, 2914 (2000).
[15] R. M. Neagu, E. Neagu, A. Kyritsis, and P. Pissis, J. Phys. D **33**, 1921 (2000).
[16] R. M. Neagu, E. Neagu, N. Bonanos, and P. Pissis, J. Appl. Phys. **88**, 6669 (2000).
[17] R. Diaz Calleja, S. Friederichs, C. Jaimes, M. J. Sanchis, J. Belana, J. C. Canadas, J. A. Diego, and M. Mudarra, Polym. Int. **46**, 20 (1998).
[18] A. Kanapitsas, P. Pissis, J. L. Gomez Ribelles, M. Monleon Pradas, E. G. Privalko, and V. P. Privalko, J. Appl. Polym. Sci. **71**, 1209 (1999).
[19] G. Georgoussis, A. Kanapitsas, P. Pissis, Yu. V. Savelyev, V. Ya. Veselov, and E. G. Privalko, Eur. Polym. J. **36**, 1113 (2000).
[20] V. V. Shilov, V. V. Shevchenko, P. Pissis, A. Kyritsis, G. Georoussis, Yu. P. Gomza, S. D. Nesin, and N. S. Klimenko, J. Non-Cryst. Solids **275**, 116 (2000).
[21] C. Cardelli, E. Tombari, and G. P. Johari, J. Phys. Chem. B **105**, 11 035 (2001).
[22] R. Casalini, A. Livi, P. A. Rolla, G. Levita, and D. Fioretto, Phys. Rev. B **53**, 564 (1996).
[23] V. Yu. Kramarenko, T. A. Ezquerra, I. Sics, F. J. Balta-Calleja, and V. P. Privalko, J. Chem. Phys. **113**, 447 (2000).
[24] V. Yu. Kramarenko, T. A. Ezquerra, and V. P. Privalko, Phys. Rev. E **64**, 051802 (2001).
[25] G. E. Roberts and E. F. T. White, in *The Physics of Glassy Polymers*, edited by R. N. Haward (Applied Science, London, 1973), p. 153.
[26] S. Havriliak and S. Negami, Polymer **8**, 161 (1967).
[27] E. M. Trukhan, Sov. Phys. Solid State **4**, 3496 (1962).
[28] V. Compan, T. S. Sorensen, R. Diaz-Calleja, and E. Riande, J. Appl. Phys. **79**, 403 (1996).
[29] C. A. Angell, J. Non-Cryst. Solids **131**, 13 (1991).
[30] C. A. Angell, Polymer **38**, 6261 (1997).
[31] A. K. Jonscher, *Dielectric Relaxation in Solids* (Chelsea Dielectric, London, 1983).
[32] A. K. Rizos, J. Alifragis, K. L. Ngai, and P. Heitjans, J. Chem. Phys. **114**, 931 (2001).
[33] A. E. Chalykh, *Diffusion in Polymer Systems* (Khimia, Moscow, 1987) (in Russian).